# Comparison of band structures and charge distributions of copper and silver

C. Y. Fong*
*Department of Physics, University of California, Davis, California 95616*

J. P. Walter† and Marvin L. Cohen‡
*Department of Physics, University of California, Berkeley, California 94720*
*and Inorganic Material Research Division, Lawrence Berkeley Laboratory, Berkeley, California 94720*

(Received 19 August 1974; revised manuscript received 13 January 1975)

The band structures of copper and silver calculated using the empirical-pseudopotential method are presented. The density of states for silver obtained from the band structure is compared with photoemission experiments. The charge distributions of the two metals were calculated in the (100) plane. A comparison of the distributions is made with reference to the results of the band structures.

## I. INTRODUCTION

The feasibility of obtaining good quality single crystals of noble metals has motivated many experimental studies on these crystals. Among these studies, optical and photoemission experiments have contributed significantly to our understanding of the electronic properties of these materials. Ehrenreich and Philipp[1] performed the first systematic measurements of the optical spectra for these metals with $0 \leq \hbar\omega \leq 24$ eV. To experimentally determine the origins of the structures in the spectrum of copper, Gerhardt[2] measured the change of the reflectivity by applying strains along different directions in the sample. Recently, the wavelength-modulation technique has also been applied to optical studies of the noble metals.[3,4] As for the uv photoemission experiments, Berglund and Spicer[5] have performed detailed studies on Cu and Ag. Later, Krolikowski and Spicer[6] improved the measurements on Cu and Ag and extended their measurements to Au. More recently, Smith[7] used the derivative technique to measure the energy distribution curves of the noble and transition metals. The energies of the structures in the spectra were accurately determined. The results obtained from both optical and photoemission measurements provided information about the relative energies of the valence and conduction bands and the density of states of the valence bands.

The first complete band structure of a noble metal was calculated by Segall[8] for Cu by using the Green's-function method. Burdick[9] calculated the band structure of Cu by the argumented-plane-wave method (APW) with the potential originally obtained by Chodorow.[10] Band structures of both Cu and Ag were calculated by Snow[11] by using the self-consistent APW method. The nonrelativistic and relativistic band structures of Ag have also been calculated by Christensen.[12] Most of these results have been compared to the results of photoemission data.

To understand the optical spectra, Ehrenreich and Philipp[1] have used the band structure of Segall to make a qualitative identification of the structure in their spectra. Later, Mueller and Phillips[13] proposed a combined interpolation scheme of the pseudopotential method and the tight-binding method. The wave functions obtained from this method were used to calculate the dipole matrix elements. There were discrepancies between the theory and the experiment, especially in the low-energy region. Two of the present authors have added to the local-pseudopotential method a $l=2$ nonlocal pseudopotential[14] to calculate the band structures of Cu and Ag by fitting to the photoemission data and the optical gap of Cu determined by Gerhardt. We also used the actual wave functions instead of the pseudo-wave-functions to calculate the dipole moments. The results agree reasonably well with the experimental data and show that most of the structure in the optical spectra of noble metals is still primarily due to one-electron processes. The same conclusion was reached later by Williams *et al.*[15] by using the Korringa-Kohn-Rostoker method.

As we discussed above, most efforts on studies of the electronic properties of Cu and Ag were concentrated on the optical properties and the photoemission data. There are, however, some x-ray measurements and calculations of form factors on Cu,[16,17] but there is a scarcity of information about the bonding properties of these metals. Charge-density studies have been made on semiconductors,[18] simple metals,[19] layer compounds,[20] and transition-metal compounds.[21] This paper represents the first attempt for charge-density calculations in noble metals. Since the band structures of Cu and Ag obtained by the empirical-pseudopotential method (EPM) agree reasonably with the optical

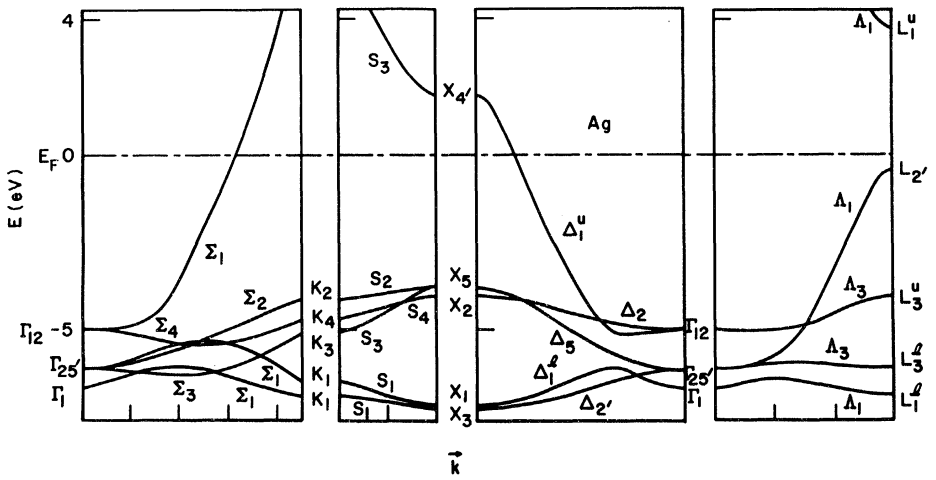


FIG. 1. Band structure of Ag.

and photoemission data, the pseudo-wave-functions, except the ones relating to $s$ and $p$ bands near the atomic site, can be considered to be reasonably accurate for calculating the charge distributions of these metals. It is hoped that these calculations will stimulate experimental investigations in this area. We present here the charge densities of Cu and Ag and make comparisons between the two metals by using the calculated band structures. The band structure of Ag calculated by the empirical-pseudopotential method has not been given elsewhere. We shall discuss the band structure of the two metals with emphasis on the results of Ag in Sec. II. In Sec. III, the charge distribution of six individual bands and the total densities of the occupied states will be presented. A comparison between the distribution of these two noble metals will also be made.

## II. BAND STRUCTURES OF SILVER AND COPPER

The band structure of Ag along different symmetry lines is plotted in Fig. 1. The optical spectrum of Ag calculated from this band structure shows a difference of 0.22 eV from experiment in the position of the minimum for $R'(\omega)/R(\omega)$.[4] This difference was attributed to the fact that we have fitted the pseudopotential to the photoemission data. The density of states obtained from this band structure is shown in Fig. 2. The Fermi level is determined by integrating the density of states to the energy corresponding to 11 electrons per unit cell. There are structures at $-4.2$, $-5.0$, $-5.2$, $-5.8$, $-6.3$, and $-6.7$ eV with respect to $E_F$, the Fermi energy. The structures reported by Smith[7] in his photoemission measurements are $-4.1$, $-4.9$, $-5.6$, $-6.2$, and $-6.9$ eV. The agreement between the theory and the experiment is of the order of 0.2 eV. The weak structure at $-5.0$ eV in the calculation is sensitive to the potential, whereas the other structures are insensitive to the potential. A comparison of a few important energy gaps with some representative first-principles calculations and the origin of the structure in the density of states are given in Tables I and II, respectively.

Since our purpose is to compare the charge distributions of Ag and Cu obtained from the results of the band-structure calculations, we include our previously reported band structure of Cu in

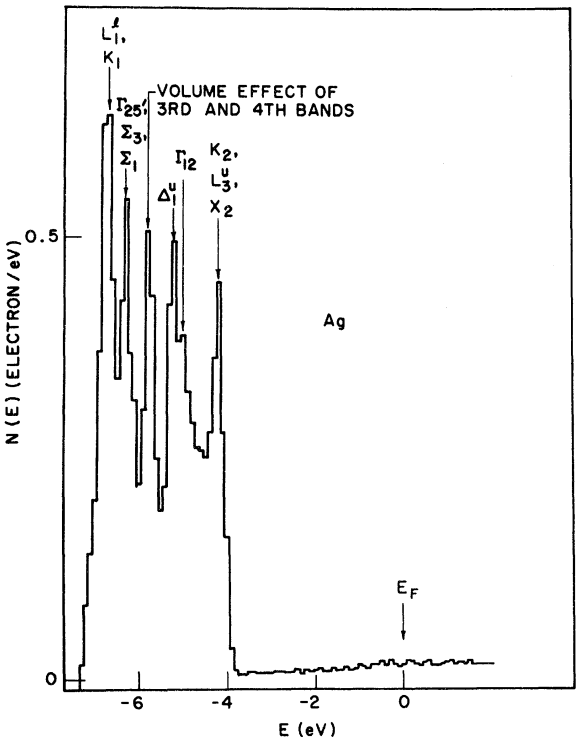


FIG. 2. Density of states of Ag.

TABLE I. A comparison of a few important energy gaps for the present results on Ag with representative first-principles calculations.

| Gaps | Energy (eV) Snow [a] self-consistent APW $\frac{5}{6}$ Slater $\rho^{1/3}$ | Christensen [b] APW $\frac{2}{3}$ Slater $\rho^{1/3}$ | Ballinger and Marshall [c] (Green's function) | Present results |
|---|---|---|---|---|
| *s-d* | | | | |
| $\Gamma_1 \rightarrow \Gamma_{25'}$ | 1.22 | 3.24 | 1.63 | 0.58 |
| $\Gamma_1 \rightarrow \Gamma_{12}$ | 2.08 | 4.34 | 2.86 | 1.74 |
| $\Gamma_1 \rightarrow X_1$ | −0.19 | 1.21 | 0.07 | −0.45 |
| $\Gamma_1 \rightarrow X_3$ | −0.05 | 1.59 | 0.14 | −0.56 |
| $\Gamma_1 \rightarrow X_2$ | 2.76 | 5.17 | 3.67 | 2.7 |
| $\Gamma_1 \rightarrow X_5$ | 3.01 | 5.36 | 3.94 | 2.96 |
| $\Gamma_1 \rightarrow L_1^l$ | 0.08 | 1.51 | 0.41 | −0.17 |
| $\Gamma_1 \rightarrow L_3^l$ | 1.18 | 3.17 | 1.77 | 0.58 |
| $\Gamma_1 \rightarrow L_3^u$ | 2.82 | 5.52 | 3.67 | 2.69 |
| *s-p* | | | | |
| $\Gamma_1 \rightarrow X_{4'}$ | 9.07 | 9.15 | 9.38 | 8.50 |
| $\Gamma_1 \rightarrow L_{2'}$ | 6.85 | 6.80 | 7.34 | 6.34 |
| $L_{2'} \rightarrow E_F$ | 0.095 | 0.76 | 0.34 | 0.44 |
| $L_{2'} \rightarrow L_1^u$ | ··· | 5.33 | 4.08 | 4.17 |

[a] Reference 11.
[b] N. E. Christensen, Phys. Status Solidi 31, 635 (1969).
[c] R. A. Ballinger and C. A. W. Marshall, J. Phys. C 2, 1822 (1969).

Fig. 3.[14] A comparison of the pseudopotentials for these two noble metals is given in Table III. There are several important differences in the two band structures: (a) The energy between the top of the $d$ bands to $E_F$ is 1.66 eV in Cu and 3.82 eV in Ag. The $d$ bands in Ag are farther away from $E_F$ than in the case of Cu. (b) The $s$-$p$ gap ($\Gamma_1 \rightarrow X_{4'}$) is 11.8 eV in Cu and 8.5 eV in Ag. (c) Because of the differences in (a) and (b), part of the $d$ band lies below the $s$-like band in Ag. It is especially clear in the $\Delta$ direction, where $\Delta_1$ and $\Delta_2'$ cross each other. This causes the $X_3$ band to be lower than $X_1$ and $\Gamma_1$. Therefore, in our calculations, the lowest band in Ag has more $d$-like character whereas in Cu it is primarily a hybridized band of the $s$ and $d$ states. From the comparison in Table I the ordering of $X_3$ and $X_1$ in the first-principles calculations is opposite to the EPM result; however, the crossing of $\Delta_1$ and $\Delta_{2'}$ is also obtained in the self-consistent APW and the Green's-function calculations. At present, there is no experimental information about this definite ordering.

TABLE II. Identifications of the structure in the density of states of Ag.

| Present calculations | Photoemission measurement | Identifications |
|---|---|---|
| −4.2 | −4.1 | $X_2$, $L_3^u$, [a] and $K_2$ |
| −5.0 / −5.2 | −4.9 | $\Gamma_{12}$ / $\Delta_1^u$ |
| −5.8 | −5.6 | Volume effect of 3rd and 4th bands |
| −6.3 | −6.2 | $\Gamma_{25'}$, $\Sigma_3$, $\Sigma_1$ |
| −6.7 | −6.9 | $L_1^l$, [a] $K_1$ |

[a] $u$ and $l$ mean upper and lower bands.

## III. CHARGE DISTRIBUTIONS OF COPPER AND SILVER

To calculate the charge distributions of the two noble metals, we have set up a mesh using 46 points in $\frac{1}{48}$ of the Brillouin zone (BZ). The wave functions are first obtained by diagonalizing the pseudopotential Hamiltonian at the $\vec{k}$ points which

TABLE III. Pseudopotential parameters of Cu and Ag.

| Pseudopotential parameters | copper | silver |
|---|---|---|
| $V$ [a] ($\lvert\vec{G}\rvert^2 = 3$) | 0.0131 Ry | 0.022 Ry |
| $V$ (4) | 0.0189 | 0.023 |
| $V$ (8) | 0.0162 | 0.0362 |
| $V$ (11) | 0.0014 | 0.0162 |
| $A_2$ | −9.9044 | −8.4610 |
| $R_M$ | 0.814 Å | 0.9447 Å |
| $\alpha$ | 0.433 | 0.43 |
| $\kappa$ | $2.63(2\pi/a)$ | $2.08(2\pi/a)$ |
| $a$ | 3.615 Å | 4.08 Å |

[a] Defined in Ref. 14.

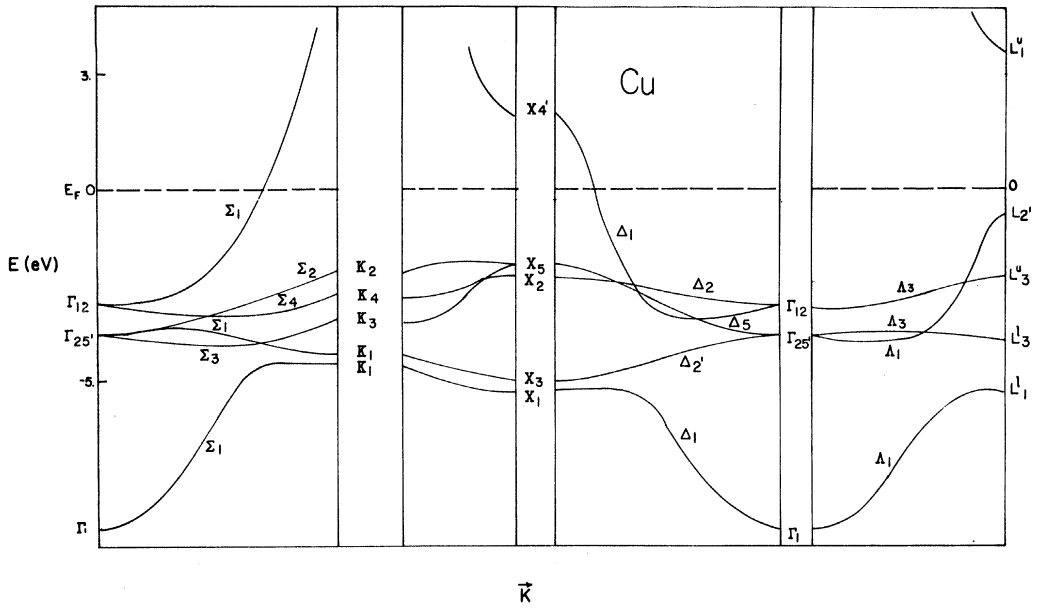


FIG. 3. Band structure of Cu.

are the center of the cube defined by the mesh. Then the 47 other wave functions were generated by the symmetry operators $\{P_R\}$ pertinent to the crystal. The charge density for each valence band can be written

$$\rho_n(\vec{r}) = \int d^3k \sum_{\{P_R\}} |\psi_{n\vec{k}}(P_R\vec{r})|^2 , \qquad (1)$$

where $\psi_{n\vec{k}}(\vec{r})$ is the wave function for the $n$th band at $\vec{k}$. The integration over $\vec{k}$ is carried out in the $\frac{1}{48}$ of the BZ. The charge distribution of a completely filled band is normalized to two electrons per band primitive cell. For the metallic crystals, at each $\vec{k}$ point the energy $E(\vec{k})$ of the partially filled conduction band should be checked, so that the distribution of the occupied states includes only contributions for $E \leq E_F$. Therefore a coarse mesh can introduce error in the distribution of the partially filled band. The total valence charge density will be the sum over $\rho_n$ of the com-

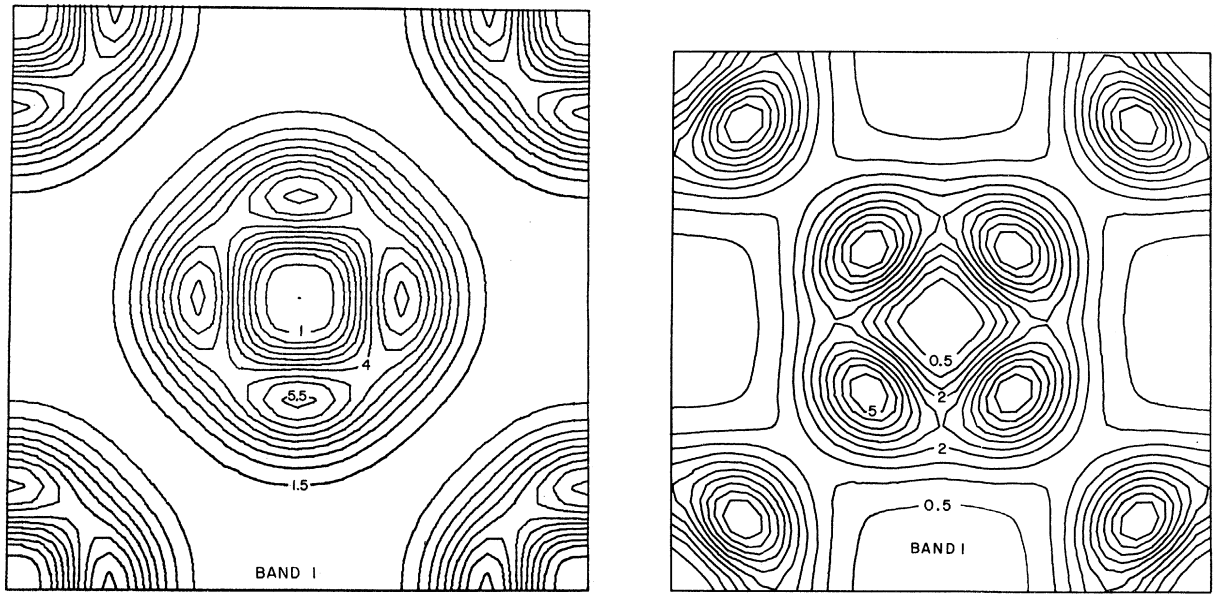


FIG. 4. (a) Charge distribution of band 1 for Cu in (100) plane. (b) Charge distribution of band 1 for Ag in (100) plane.

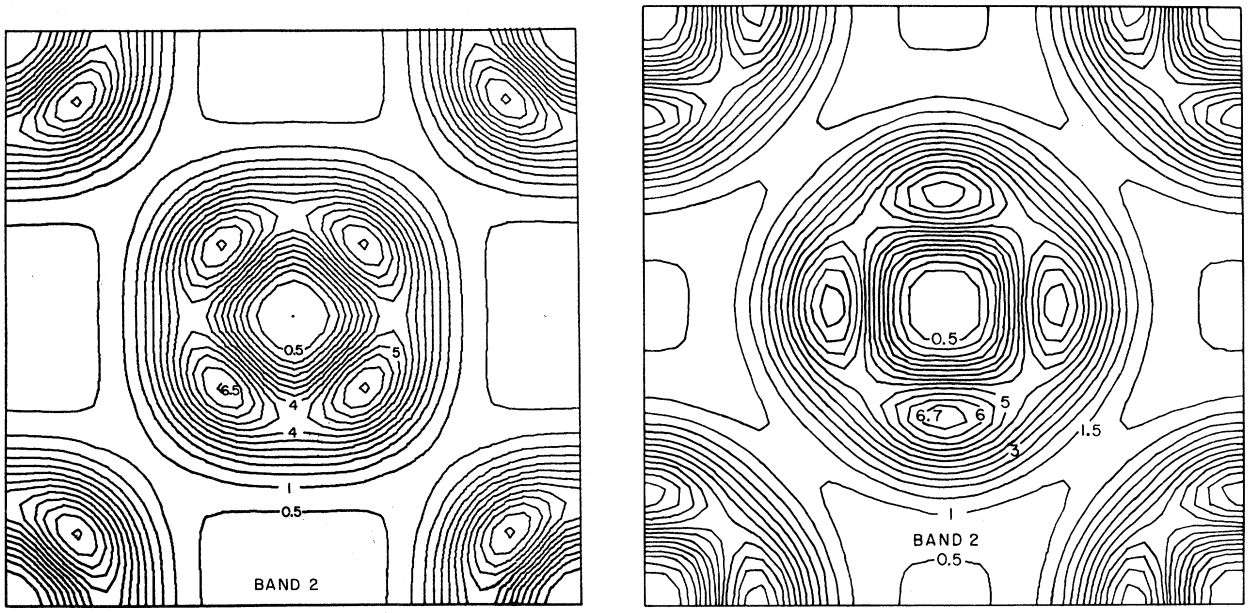


FIG. 5. (a) Charge distribution of band 2 for Cu in (100) plane. (b) Charge distribution of band 2 for Ag in (100) plane.

pletely and partially occupied bands.

In Figs. 4(a)–9(b) we have plotted the charge distributions of the individual bands which are either completely or partially occupied. The (a)'s refer to Cu, while the (b)'s refer to Ag. All these sections are in the (100) plane. The edges are in the units of their respective lattice constants. The atoms are at the corners and at the center of the plane. In Fig. 4(a), the four lobes (contours with the values close to 5.5) around the atom point along the axes of the cubic cell. These lobes are due to the hybridization of the $d$ states $(X_1, K_1, L_1^I)$ to the $s$-like states $(\Gamma_1)$. The shapes of the contours resemble the ones in Fig. 5b. The distributions in Fig. 5a are for the pure $d$-like states $(\Delta_{2'}, X_3, \Sigma_3, \Lambda_3)$. The lobes are pointing along the face diagonal. Comparing this with the results of Ag, the contours are much like the ones in Fig. 4b. This

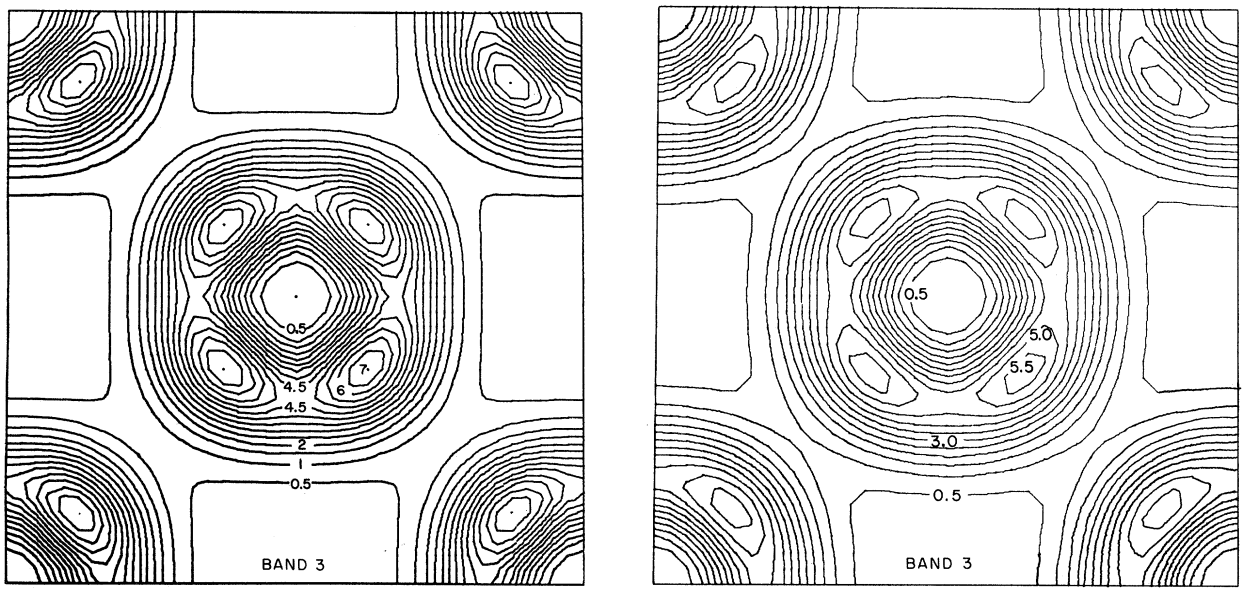


FIG. 6. (a) Charge distribution of band 3 for Cu in (100) plane. (b) Charge distribution of band 3 for Ag in (100) plane.

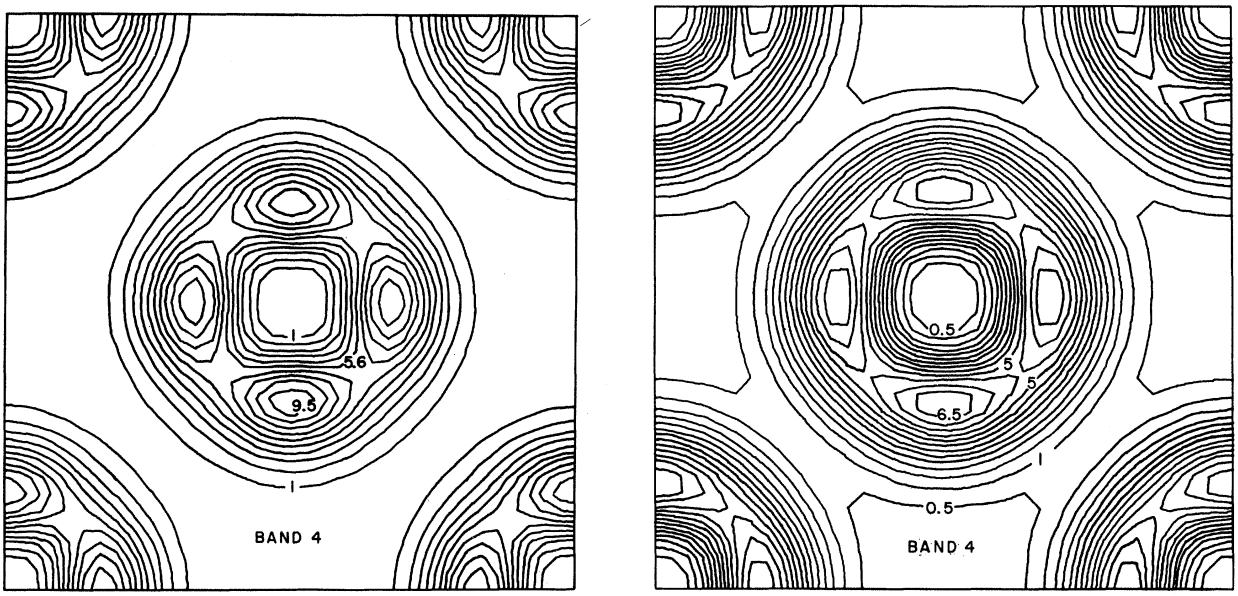


FIG. 7. (a) Charge distribution of band 4 for Cu in (100) plane. (b) Charge distribution of band 4 for Ag in (100) plane.

is due to the fact that the $X_3$ and $X_1$ bands of Ag are reversed in order and the crossing of $\Delta_1$ and $\Delta_{2'}$ happens very near $\Gamma_1$, as we discussed in Sec. III. The rest of the distributions are quite similar in shape for both cases. As the band indices increase from 3 to 5, the lobes of the $d$ states rotate back and forth by 45°; so the maximum charge of one band is located in the region where the charge density is minimum for the next-lower energy band. The pattern of this kind of configuration indicates that these charges experience most effectively the attractive potential from the nucleus and the least screening potential. Figs. 9(a) and 9(b) show the distributions of the partially occupied $d$-$p$ hybridized bands (6th band in Figs. 1 and 3). The distribution of Ag is rather uniform compared with all lower-energy bands and the corresponding case of Cu. This means there are more $d$-like states in the 6th band of Cu than in that of Ag. The larger differences in the separation of the $d$ band

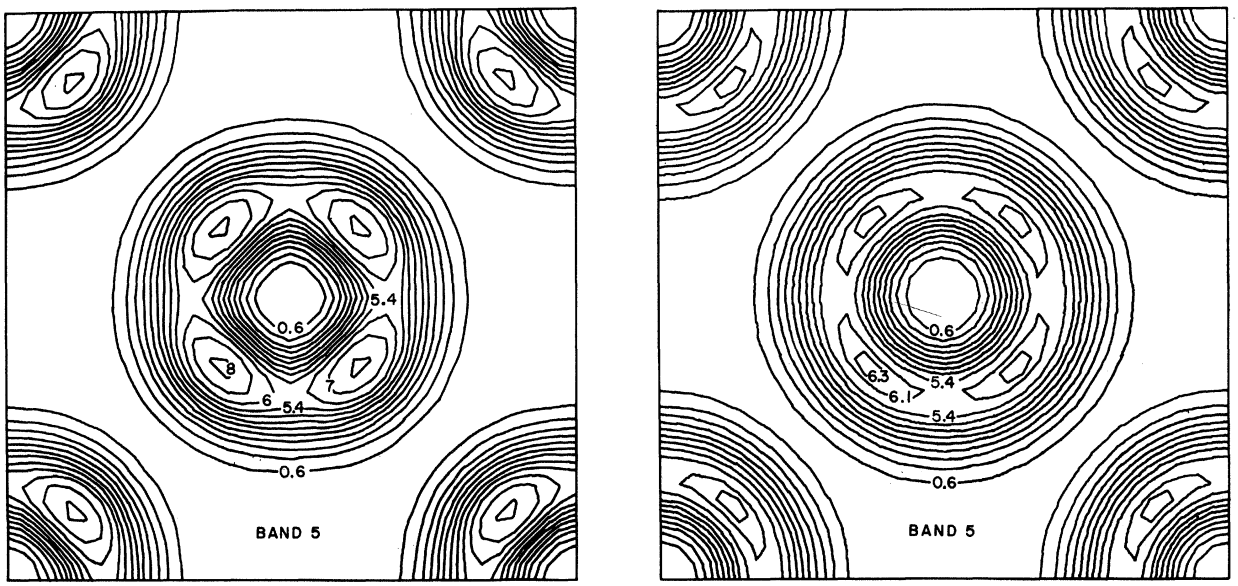


FIG. 8. (a) Charge distribution of band 5 for Cu in (100) plane. (b) Charge distribution of band 5 for Ag in (100) plane.

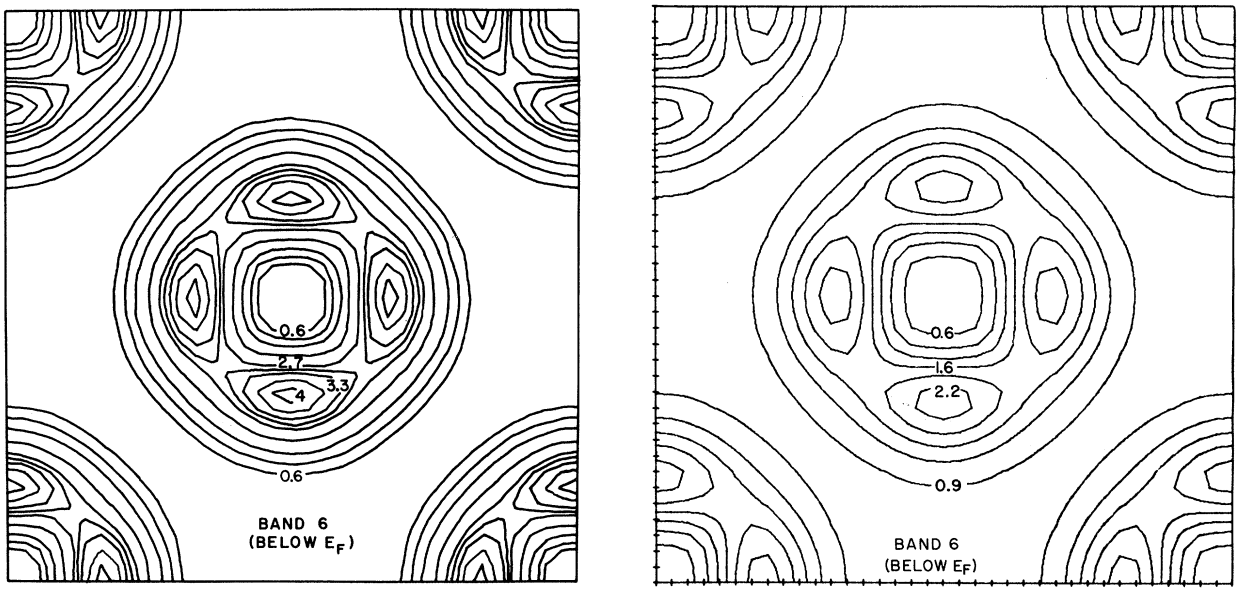


FIG. 9. (a) Charge distribution of band 6 (occupied portion) for Cu in (100) plane. (b) Charge distribution of band 6 (occupied portion) for Ag in (100) plane.

with respect to $E_F$ of Ag cause the distribution to be more like the case of simple metals.[19] The total charge of this band for both metals is about 5% more than what it should be. Since we are interested in the qualitative features of the charge density of the two noble metals, this error will not ruin the main features of the distributions. However, if a calculation of the x-ray form factors is made to compare with the x-ray data, a finer mesh is definitely needed.

The total charge distributions of the occupied states are shown in Figs. 10(a) and 10(b). The maximum of the contours associated with each atom occurs near $\frac{1}{4}$ of the interatomic distance. These are made up primarily from the lobes of the $d$ states. The contours exhibit nearly perfect spherically symmetric shape around the atom. Slight deviations happen in the regions midway

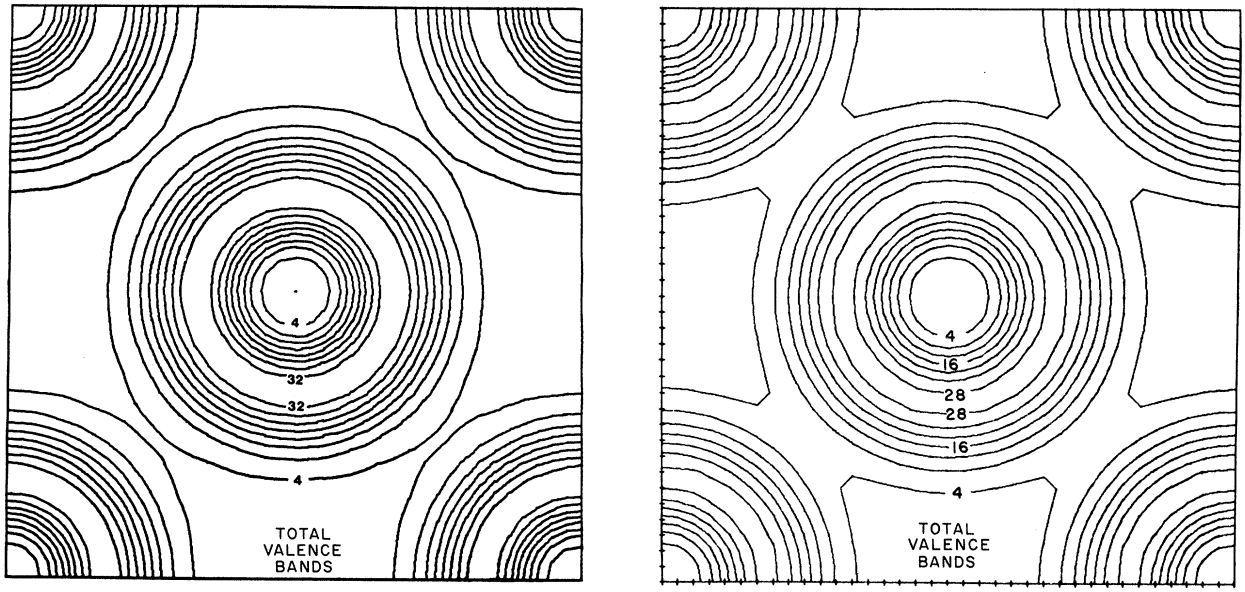


FIG. 10. (a) Total charge distribution of the occupied bands for Cu in (100) plane. (b) Total charge distribution of the occupied bands for Ag in (100) plane.

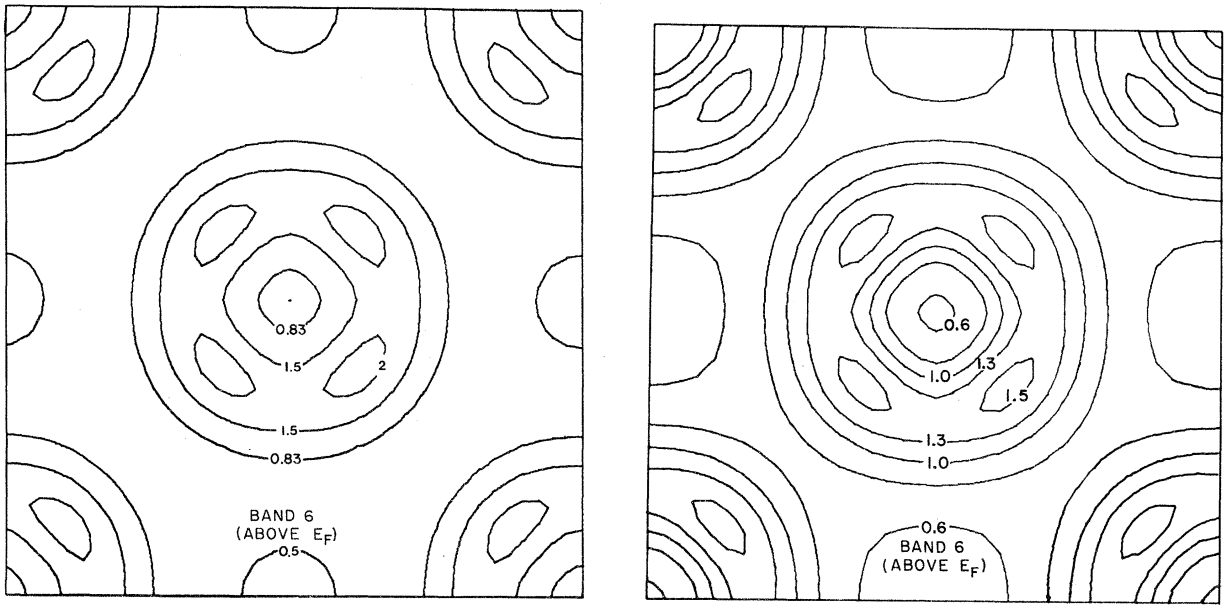


FIG. 11. (a) Charge distribution of band 6 (unoccupied portion) for Cu in (100) plane. (b) Charge distribution of band 6 (unoccupied portion) for Ag in (100) plane.

between the atoms. It is just what one would expect. The completely filled $d$ states and an additional $s$-like electron are expected to give the calculated spherical distribution for the total charge density. This also explains why the APW method using the muffin-tin potential works so well for the noble metals.

The charge distributions of the unoccupied portion of the 6th conduction band are shown in Figs. 11(a) and 11(b). The shapes of the contours and the directions which the lobes are pointing are the same for Cu and Ag. As we see in Figs. 1 and 3, the angular momentum character is the same for these bands for the two metals. The magnitudes of the contours in Figs. 11(a) and 11(b) are also comparable. The conduction bands of the two metals as suggested here are quite similar. As we mentioned earlier, the charge distributions of these $s$-$p$ states, within a radius of $\frac{1}{10}$ of the side of the square around the atoms, are not expected to be accurate, because the pseudo-wave-functions are used in the calculations. The total charges for these two cases are 5% less than what they should be, so the sums of the charges in Figs. 9(a), 11(a) and 9(b), 11(b) give two electrons per band primitive cell.

In summary, we have presented the band structure of Ag calculated by the EPM and compared it with the one of Cu. The density of states derived from the band structure of Ag gives reasonable agreement to the photoemission data. The electronic charge distributions for Cu and Ag have been calculated in the (100) plane using the pseudo-wave-functions from the band structures. The effect of the crossover of the $X_1$ and $X_3$ bands in Ag is manifested in the charge distributions of the *individual* bands. Furthermore, because the $d$ bands in Ag are about 4 eV below $E_F$, whereas in Cu the separation is about 2 eV, the charge distributions show clearly that there is a stronger mixing of the $d$ states with the $s$ state in the lower energy bands and a smaller hybridization effect for the 6th band in Ag. Except for the distributions of the second and the third bands in Cu, the lobes of the $d$ states rotate 45° back and forth as the band indices change; so the $d$ states experience the strongest possible attractive potential from the nucleus. The features of the distributions of the $d$ states should be more accurately represented than the ones of the $s$ and $p$ states near the atomic site because the detailed nature of the $d$ states has been taken into account by the $l=2$ nonlocal pseudopotential.

## ACKNOWLEDGMENT

Part of this work was done under the auspices of the U.S. Atomic Energy Commission.

*Supported in part by the U.S. Air Force Office of Scientific Research (AFSC) under Grant No. AFOSR-72-2353.

†Present address: 1160 NW North River Drive, Miami, Fla. 33136.

‡Supported in part by the National Science Foundation Grant No. GH35688.

[1]H. Ehrenreich and H. R. Philipp, Phys. Rev. 128, 1622 (1962).
[2]U. Gerhardt, Phys. Rev. 172, 651 (1968).
[3]C. Y. Fong, M. L. Cohen, R. R. L. Zucca, J. Stokes, and Y. R. Shen, Phys. Rev. Lett. 25, 1486 (1970).
[4]J. Stokes, Y. R. Shen, Y. W. Tsang, M. L. Cohen, and C. Y. Fong, Phys. Lett. 38, 347 (1972).
[5]C. N. Berglund and W. E. Spicer, Phys. Rev. 136, A1030 (1964).
[6]W. F. Krolikowski and W. E. Spicer, Phys. Rev. 185, 882 (1969); B 1, 478 (1970).
[7]N. V. Smith, Phys. Rev. B 3, 1892 (1970); B 9, 1365 (1974).
[8]B. Segall, Phys. Rev. 125, 109 (1962).
[9]G. A. Burdick, Phys. Rev. 129, 138 (1963).
[10]M. Chodorow, Phys. Rev. 55, 675 (1939).
[11]E. C. Snow, Phys. Rev. 171, 785 (1968); 172, 708 (1968).
[12]N. E. Christensen, Phys. Status Solidi 54, 551 (1972).
[13]F. M. Mueller and J. C. Phillips, Phys. Rev. 157, 600 (1967).
[14]C. Y. Fong and M. L. Cohen, Phys. Rev. Lett. 24, 306 (1970).
[15]A. R. Williams, J. F. Janak, and V. L. Moruzzi, Phys. Rev. Lett. 28, 671 (1972).
[16]R. J. Temkin, V. E. Henrich, and P. M. Raccah, Phys. Rev. B 6, 3572 (1972).
[17]F. J. Arlinghaus, Phys. Rev. 153, 743 (1967).
[18]M. L. Cohen, Science 179, 1189 (1973); and references therein.
[19]J. P. Walter, C. Y. Fong, and M. L. Cohen, Solid State Commun. 12, 3031 (1973).
[20]C. Y. Fong and M. L. Cohen, Phys. Rev. Lett. 32, 720 (1974).
[21]D. J. Chadi and M. L. Cohen, Phys. Rev. B 10, 496 (1974).